UC Berkeley

UC Berkeley Previously Published Works

Title

Transcriptional activation of lipogenesis by insulin requires phosphorylation of MED17 by CK2

Permalink

https://escholarship.org/uc/item/22r8d9c8

Journal

Science Signaling, 10(467)

ISSN

1945-0877

Authors

Viscarra, Jose A
Wang, Yuhui
Hong, Il-Hwa
et al.

Publication Date

2017-02-21

DOI

10.1126/scisignal.aai8596

Peer reviewed

eScholarship.org Powered by the California Digital Library
University of California

Author Manuscript

Author Manuscript

Author Manuscript

Author Manuscript

HHS Public Access

Author manuscript

Sci Signal. Author manuscript; available in PMC 2017 August 21.

Published in final edited form as:

Sci Signal. ; 10(467): . doi:10.1126/scisignal.aai8596.

Transcriptional Activation of Lipogenesis by Insulin Requires Phosphorylation of MED17 by CK2*

Jose A. Viscarra, **Yuhui Wang**, **Il-Hwa Hong**[1], and **Hei Sook Sul**[2]

Department of Nutritional Sciences and Toxicology, University of California, Berkeley, CA 94720

Abstract

De novo lipogenesis is precisely regulated by nutritional and hormonal conditions. The genes encoding various enzymes involved in this process, such as fatty acid synthase (FASN), are transcriptionally activated in response to insulin. Here we showed that USF1, a key transcription factor for *FASN* activation, directly interacted with the Mediator subunit MED17 at the *FASN* promoter. This interaction recruited Mediator, which can bring POL II and other general transcription machinery to the complex. Moreover, we showed that MED17 was phosphorylated at Ser^{53} by casein kinase 2 (CK2) in the livers of fed mice or insulin-stimulated hepatocytes, but not in the livers of fasted mice or untreated hepatocytes. Furthermore, activation of the *FASN* promoter in response to insulin required this CK2-mediated phosphorylation event, which occurred only in the absence of p38 MAPK-mediated phosphorylation at Thr^{570}. Overexpression of a non-phosphorylatable S53A MED17 mutant or knockdown of MED17, as well as CK2 knockdown or inhibition, impaired hepatic de novo fatty acid synthesis and decreased triglyceride content in mice. These results demonstrate that CK2-mediated phosphorylation of Ser^{53} in MED17 is required for the transcriptional activation of lipogenic genes in response to insulin.

INTRODUCTION

De novo lipogenesis is a metabolically expensive process that is tightly coupled to nutritional and hormonal state(1). In fasting, glucagon secretion in response to low glucose in the circulation promotes gluconeogenesis while suppressing lipogenesis in liver, through a pathway that involves the glucagon receptor, cyclic AMP (cAMP), protein kinase A (PKA), and p38 mitogen-activated protein kinase (p38 MAPK) (2). In contrast, after feeding,

*This manuscript has been accepted for publication in Science Signaling. This version has not undergone final editing. Please refer to the complete version of record at http://www.sciencesignaling.org/. The manuscript may not be reproduced or used in any manner that does not fall within the fair use provisions of the Copyright Act without the prior, written permission of AAAS.

[2]Corresponding Author: hsul@berkeley.edu.

[1]Present address: Department of Pathology, College of Veterinary Medicine, Gyeongsang National University, Jinju 52828, Republic of Korea

AUTHOR CONTRIBUTIONS:

JAV, YW, and HSS designed the study; JAV, YW and IH conducted experiments; JAV and HSS interpreted data and wrote the paper; all authors discussed the results and approved the final manuscript.

COMPETING INTERESTS:

The authors declare that they have no competing interests.

DATA AND MATERIALS AVAILBILITY:

The mass spectrometry phosphoproteomics data have been deposited to the MassIVE server maintained by the Center for Computational Mass Spectrometry at UCSD with the dataset identifier MSV000080324 and MSV000080325.

Author Manuscript Author Manuscript Author Manuscript Author Manuscript

especially a high carbohydrate diet, increased glucose concentration in the circulation triggers the secretion of insulin which induces the conversion of excess glucose to fatty acids and fat by coordinately activating numerous lipogenic genes at the transcriptional level. Fatty acid synthase (FASN) is a central enzyme in de novo lipogenesis. Because FASN is regulated primarily at the transcriptional level, it provides an ideal system to assess the transcriptional activation of lipogenesis in response to insulin(3, 4).

We have reported that the binding of upstream stimulatory factor 1 (USF1) to the -65 enhancer box (E-box) is required for the activation of the *FASN* promoter in response to insulin (5–10). Mice lacking USF1 exhibit impaired induction of *FASN*(11). Unlike the genes encoding some of the transcription factors involved in lipogenesis, such as sterol regulatory element-binding protein 1c (*SREBP1c*), *USF1* is constitutively expressed. We have found that insulin activates the *FASN* promoter by USF1 through several pathways that result in the phosphorylation and acetylation of USF1(12, 13). USF1 acts as a molecular switch and hub for transcription factor and coregulator recruitment for transcriptional activation in response to insulin. However, RNA polymerase II (POL II) and general transcription machinery ultimately must be recruited to the promoter regions. In this regard, Mediator, a large multi-subunit complex conserved across all eukaryotes, connects gene-specific transcription factors to the POL II preinitiation complex(14–16). Certain Mediator subunits directly interact with transcription factors that recruit Mediator to specific DNA sites (14, 17, 18). However, signaling pathways and posttranscriptional modifications of specific Mediator subunits in response to different physiological conditions to regulate transcription have not been well studied.

Here we showed that USF1 directly interacted with Mediator subunit 17 (MED17). Moreover, in response to insulin, MED17 was phosphorylated at Ser^{53} by casein kinase 2 (CK2) only in the absence of p38 MAPK-mediated phosphorylation at Thr^{570}, allowing recruitment of MED17 and thus Mediator for the transcriptional activation of lipogenesis in response to insulin.

RESULTS

USF1 directly interacts with MED17

We have previously reported that USF1 functions as a central hub of transcription factors and coregulators for transcriptional activation of lipogenic genes in response to insulin. Since Mediator complex needs to be recruited to the promoter region to initiate transcription, we tested whether USF1 interacts with specific mediator subunits to recruit Mediator. We examined various Mediator subunits, including MED15, MED21, MED25, and MED28, which have previously been reported to interact with transcription factors (Fig. S1). Here, we identified MED17 as a direct interacting partner of USF1. Immunoprecipitation analysis of 293FT cells expressing USF1 and MED17 using an antibody against USF1 or MED17 revealed a strong interaction between USF1 and MED17 (Fig. 1A). This interaction was also detected in co-immunoprecipitation experiments using antibodies against the epitope tags on USF1 and MED17 (Fig. 1A). We also detected an interaction between endogenous USF1 and MED17 in co-immunoprecipitation experiments using nuclear extracts prepared from livers of mice (Fig. 1B). Glutathione S-transferase (GST) pulldown experiments showed that

Author Manuscript Author Manuscript Author Manuscript Author Manuscript

in vitro transcribed and translated MED17 was precipitated by full-length GST-USF1 fusion proteins, showing that USF1 directly interacted with MED17 (Fig. 1C).

We next used GST-pulldown assays to identify the domains of USF1 and MED17 involved in the interaction. Whereas deletion of the basic helix loop helix (bHLH) or the leucine zipper (LZ) domains of USF1 did not affect the USF1-MED17 interaction, deletion of the activation domain of USF1 completely prevented the pulldown of MED17. Furthermore, the activation domain of USF1 was sufficient for interaction with MED17. These results indicated that MED17 directly interacted with the activation domain of USF1 (Fig. 1C). Because the domain structure of mammalian MED17 has not been determined, we used the yeast MED17 as a guide in creating MED17 deletion constructs (19). Polyhistidine-tag (His-tag) pulldown assays of USF1 revealed that deletion of the C-terminal domain (CTD), but not that of the N-terminal domain (NTD) or the bundle domain (BD), prevented the pulldown of USF1 (Fig. 1D) and that the CTD by itself showed interaction with USF1, demonstrating that the CTD of MED17 was sufficient for interaction with USF1. Overall, we concluded that the activation domain of USF1 directly interacted with the CTD of MED17.

Next, we examined the functional importance of the MED17-USF1 interaction. *FASN* promoter-driven luciferase activity was increased by USF1 transfection, as we reported previously (12, 13) (Fig. 1E). Moreover, cotransfection of MED17 with USF1 further increased the *FASN* promoter activity in a dose-dependent manner (Fig. 1E), whereas MED17 alone did not show an appreciable effect. These results suggested that, through interaction with USF1, MED17 activated the *FASN* promoter. Indeed, despite being sufficient for the physical interaction with USF1 (Fig. 1D), transfection of the MED17 CTD was as ineffective as the MED17 NTD in activating the *FASN* promoter (Fig. 1F). While the construct containing the MED17 CTD and BD activated the promoter about 25% more than USF, it did not activate as much as wild-type MED17 (Fig.1F), suggesting that full length MED17 was required for proper promoter activation.

MED17 is Recruited to the *FASN* promoter in a feeding- and insulin-dependent manner

We next performed chromatin immunoprecipitation (ChIP) to assess MED17 occupancy of the -444 *FASN* promoter-luciferase reporter. We detected increased enrichment of MED17 at the *FASN* promoter region when MED17 was cotransfected with USF1 (Fig. 2A). Although short interfering RNA (siRNA)-mediated knockdown only resulted in approximately 40% reduction in *USF1* mRNA abundance (Fig. S2A), USF1 siRNA transfection reduced enrichment of not only USF1, but also MED17 at the *FASN* promoter region (Fig. 2B). We also examined the enrichment of endogenous MED17 at the -444 *FASN* promoter and detected higher enrichment in the presence USF1, and lower enrichment upon knockdown of USF1 (Fig. S2C). We also used the -444 *FASN* promoter construct containing the -65 E-box mutation that prevents USF1 binding(13). Indeed, we detected reduced enrichment of not only USF1, but also MED17 in cells cotransfected with the mutant construct, compared to cells cotransfected with the wild-type *FASN* promoter construct (Fig. 2C). Recruitment of MED17 was reduced in cells cotransfected with the MED17 C-terminal helix (CTH) deletion construct, which could not interact with USF1

Author Manuscript Author Manuscript Author Manuscript Author Manuscript

(Fig. S2B), compared to cells cotransfected with wild-type MED17 (Fig. 2D). Overall, these experiments demonstrated that the binding of MED17 to the *FASN* promoter required interaction between MED17 and USF1, as the absence of USF1 binding or loss of interaction with USF1 prevented MED17 recruitment to the *FASN* promoter. ChIP analysis of the endogenous *FASN* gene in HepG2 cells revealed the enrichment of USF1 at the proximal promoter region, near the -65 E-box and -332 E-box regions as we previously reported(6, 10, 13) (Fig. 2E left), and MED17 binding to be highest at the proximal *FASN* promoter, especially at the -65 E-box region. Similarly, RNA POL II occupancy was highest at the proximal *FASN* promoter.

ChIP analysis detected USF1 at the *FASN* promoter region in both insulin-treated or untreated HepG2 cells, whereas MED17 and POL II were bound to the *FASN* promoter only in insulin-treated HepG2 cells (Fig. 2E middle and right). We performed sequential ChIP (Re-ChIP) using the USF1 antibody followed by the MED17 antibody, which showed that MED17 bound at the *FASN* promoter region only in insulin-treated cells. These results further demonstrated that USF1 recruited MED17 to the *FASN* promoter in response to insulin treatment (Fig. 2E middle and right). We next examined by ChIP analysis whether MED17 was recruited to other lipogenic promoters. As expected, recruitment of total USF1 was not altered by the presence or absence of insulin (Figure 2F left). In contrast, insulin treatment of HepG2 cells increased the recruitment of MED17 to the promoter regions of various lipogenic genes, but not those of fatty acid oxidative enzymes, such as acyl-CoA oxidase (*ACOX)* or acetyl-CoA acyltransferase 1 (*ACAA1)* (Fig. 2F middle). A similar increase in POL II recruitment to the lipogenic promoters was detected upon insulin treatment (Fig. 2F right). Furthermore, we also detected recruitment of other Mediator subunits, namely MED6 and MED7, in HepG2 cells, reflecting the recruitment of the Mediator complex to the lipogenic genes through the direct interaction of MED17 with USF1 (Fig. S3). ChIP analysis revealed that USF1 occupancy at lipogenic or fatty acid oxidative promoters in mouse liver was not altered by fasting or refeeding (Fig. 2G left). In contrast, MED17 and POL II were enriched at the proximal promoter regions of fatty acid synthetic genes, such as *FASN*, acetyl-CoA carboxylase 1 (*ACC1)*, ATP citrate lyase (*ACLY)*, and *SREBP1c*, but not fatty acid oxidative genes, in refed mouse livers (Fig. 2G middle and right). Overall, these results showed that MED17 and thus the Mediator complex was recruited to the promoter regions of lipogenic genes in response to insulin exposure in cells or feeding in mice.

Differential phosphorylation of MED17 is required for *FASN* promoter activation

Since neither *MED17* mRNA nor MED17 protein abundance was affected by fasting or feeding in mice or by the presence or absence of insulin in cells (Fig. S4), we hypothesized that posttranslational modification of MED17 may be required for its recruitment and activation of lipogenic genes in response to insulin. We assessed MED17 phosphorylation status in the livers of fasted or fed mice. Immunoblotting of MED17 immunoprecipitates with a phospho-serine antibody revealed increased phosphorylation of MED17 in the refed, compared to the fasted state (Fig. S5). To identify the phosphorylation sites in MED17, we performed mass spectrometric (MS) analysis of serum starved or insulin treated cells overexpressing MED17. We detected phosphorylation of Thr^{570} only in lysates from serum

Author Manuscript Author Manuscript Author Manuscript Author Manuscript

starved, but not from insulin treated cells. In addition, a Phospho.Elm database search indicated that Ser^{53} and Ser^{55} were phosphorylated in both mice and humans in multiple proteomic analyses. We therefore tested whether the phosphorylation of any of these sites of MED17 affected *FASN* promoter activity using expression vectors containing alanine or aspartate mutants of Ser^{53}, Ser^{55}, and Thr^{570}, to mimic hypophosphorylation or hyperphosphorylation, respectively. Compared to wild-type MED17, the S53A mutant showed significantly lower luciferase activity in response to insulin in cells cotransfected with USF1, whereas the S53D retained the same degree of activation as wild-type MED17 (Fig. 3A), suggesting that phosphorylation of Ser^{53} in MED17 enhanced *FASN* promoter activation. Ser^{55} was eliminated as a candidate phosphorylation site, since neither S55A nor S55D mutants showed a similar degree of activation as wild-type MED17 (Fig. 3A). In contrast, while the wild-type and T570A MED17 mutant activated the *FASN* promoter upon cotransfection with USF1, the T570D mutant did not increase luciferase activity to the same degree as wild-type MED17 (Fig. 3B), suggesting that phosphorylation of Thr^{570} in the absence of insulin suppressed *FASN* promoter activity.

Because we were interested in examining *FASN* promoter activation by MED17 in response to insulin, we generated an anti-phosphopeptide antibody specific for the Ser^{53} site of MED17. Immunoblotting with this Ser^{53} phospho-specific antibody showed that Ser^{53} in MED17 in livers was phosphorylated to a greater extent in fed mice than in fasted mice (Fig. 3C left). The phosphorylation of Ser^{53} in MED17 was also substantially increased in insulin-treated compared to serum-starved HepG2 cells (Fig. 3C right). Overall, these results suggested that, in contrast to the phosphorylation of Thr^{570} in MED17 that occurred in the absence of insulin, MED17 was phosphorylated at Ser^{53} upon feeding or insulin treatment, an indication that this differential MED17 phosphorylation event may regulate *FASN* promoter activity.

Casein Kinase 2 Phosphorylates MED17 at Ser^{53}, which is prevented by phosphorylation of Thr^{570} by p38 MAPK

We used kinase prediction software (GPS2.1)(20) to identify potential candidate kinases that catalyze the phosphorylation of MED17. Thr^{570}, the site that was phosphorylated in serum starved samples, was a potential target site of p38 MAPK, which is activated in livers of fasted mice(2, 21, 22). By in vitro kinase assay, we detected phosphorylation of Thr^{570} in wild-type MED17 but not the T570A mutant by p38 MAPK using phospho-threonine specific antibody (Fig. S6). Ser^{53}, the site that was phosphorylated in response to insulin, was predicted to be a consensus Casein Kinase 2 (CK2) target. Although CK2 is involved in many biological functions and works in similar pathways as insulin, the regulation of this kinase is not well understood. (23, 24). Immunoblotting of in vitro kinase assays with the P-Ser^{53} phospho-specific antibody revealed phosphorylation of wild-type and the S55A mutant form of MED17, but not the S53A mutant, thus indicating Ser^{53} was a target site for CK2 (Fig. 4A). These results were confirmed with ProQ Diamond phospho-specific staining, demonstrating that CK2 phosphorylated the MED17 wild-type and S55A mutant proteins but not the S53A mutant protein. (Fig. 4A). Moreover, treatment with the CK2 inhibitor CX-4945 completely blocked phosphorylation of Ser^{53} (Fig. 4A). In cultured cells, the phosphorylation of overexpressed MED17 at Ser^{53} increased upon transfection with CK2 α

Author Manuscript Author Manuscript Author Manuscript Author Manuscript

and β (Fig. 4B). Overall, these results demonstrated that Ser^{53} of MED17 was phosphorylated by CK2.

Unlike wild-type or the T570A mutant of MED17, the T570D mutant did not activate the *FASN* promoter in luciferase reporter assays (Fig. 3B), prompting us to assess the relationship between phosphorylation of Thr^{570} and Ser^{53} in MED17. Cotransfection of CK2 increased the phosphorylation of Ser^{53} of wild-type MED17, but not that of the T570D mutant (Fig. 4C), suggesting that the phospho-mimicking T570D mutation prevented phosphorylation of Ser^{53} by CK2. Since we detected phosphorylation of the p38 MAPK site Thr^{570} only in serum starved cells, these data support the idea that CK2 could not phosphorylate MED17 in the absence of insulin when MED17 was phosphorylated at Thr^{570}. Indeed, MED17 phosphorylation at Ser^{53} was detected in HepG2 cells upon insulin treatment, which was prevented by the CK2 inhibitor CX-4945 (Fig. 4D). However, in the absence of insulin, Ser^{53} was not phosphorylated either in the absence or presence of the CK2 inhibitor. Overall, we demonstrated that, although CK2 is generally thought to be constitutively active, CK2-mediated phosphorylation of MED17 at Ser^{53} occurred only in the presence of insulin when Thr^{570} was not phosphorylated. Thus, this phosphorylation event provides a means to regulate CK2 action.

CK2-mediated phosphorylation of MED17 at Ser^{53} is required for its recruitment and activation of the *FASN* promoter in response to insulin

We sought to determine the role of CK2 in the activation of the *FASN* promoter. CK2 cotransfection significantly enhanced activation of the *FASN* promoter in cells expressing wild-type MED17, but not in those expressing the S53A mutant (Fig. 4E). These results demonstrated that CK2-mediated phosphorylation of Ser^{53} activated the *FASN* promoter. The CK2 specific inhibitor CX-4945 significantly impaired the induction of *FASN* and other lipogenic genes, such as mitochondrial glycerol-3-phosphate acyltransferase (*GPAM), ACC*, and *SREBP1c* in response to insulin in HepG2 cells. However, expression of the oxidative gene *ACOX* was not affected by insulin treatment either in the presence or absence of CX-4945 (Fig. 4F). Finally, we also found that short hairpin RNA (shRNA) mediated knockdown of MED17 or CK2 significantly reduced triglyceride accumulation in HepG2 cells (Fig. S7).

We next tested the requirement of phosphorylation of Ser^{53} in MED17 for its recruitment to the *FASN* promoter region. ChIP analysis indicated that in HepG2 cells, insulin treatment did not affect USF1 binding to the *FASN* promoter region. In contrast, insulin treatment increased enrichment of wild-type MED17, but not the S53A mutant, at the *FASN* promoter region (Fig. 4G), indicating that MED17-mediated phosphorylation at Ser^{53} was required for its recruitment to the *FASN* promoter region. CX-4945 treatment greatly reduced the enrichment of MED17 at the *FASN* promoter region in HepG2 cells (Fig. 4H), further demonstrating that phosphorylation by CK2 was required for MED17 recruitment to the *FASN* promoter. We next tested whether CK2 itself was recruited to the *FASN* promoter. ChIP analysis revealed greater CK2 binding at the *FASN* proximal promoter region upon insulin treatment, as well as Ser^{5} phosphorylation of POL II CTD at the promoter region and Ser^{2} phosphorylation of POL II at the 8500 base pair (bp) region within the *FASN* gene (Fig.

Author Manuscript Author Manuscript Author Manuscript Author Manuscript

4I), indicating transcription initiation as well as elongation of the *FASN* transcript in response to insulin(25). However, we detected CK2 recruitment only at the *FASN* promoter region, and not in the intragenic region, suggesting that the role of CK2-mediated phosphorylation of MED17 was to recruit Mediator for *FASN* transcription initiation.

Phosphorylation of Ser^{53} in MED17 is required for lipogenesis by insulin in vivo

We sought to examine the role of phosphorylation of Ser^{53} by CK2 on the transcription of *FASN* and other lipogenic genes. Transduction of the S53A mutant MED17-expressing adenovirus into HepG2 cells (Fig. 5A left and middle) resulted in significantly reduced the expression of genes encoding enzymes involved in fatty acid and fat synthesis, such as *FASN, GPAM, ACC* and *SREBP1c*, while not affecting that of oxidative genes, such as *ACOX* and *ACAA1* (Fig. 5A right). Tail vein injection of the MED17 S53A adenovirus (Fig. 5B left and middle) reduced hepatic mRNA abundance over 70% for genes involved in fatty acid and fat synthesis, including *FASN, SREBP1c, ACC1* AND *ACLY*, but not that of oxidative genes, such as *ACOX1* and *ACAA1B* (Fig. 5B right). We also detected an approximately 50% lower FASN protein content in S53A infected livers (Fig. S9C). Newly synthesized palmitate was reduced in the livers of mice infected the S53A adenovirus, demonstrating that the decreased expression of fatty acid and fat synthesis genes impaired hepatic de novo fatty acid synthesis (Fig. 5C left). Triglyceride contents in the livers of these mice were also reduced (Fig. 5C right). Thus, S53A overexpression impaired lipogenic gene activation, probably by acting in a dominant negative manner, since overexpression of wild-type MED17 resulted in increased mRNA abundance of lipogenic genes in HepG2 cells and in livers of mice in vivo (Fig. S8A and B). We also detected higher triglyceride content in the livers of these mice (Fig. S8B).

We next hypothesized that if phosphorylation of Ser^{53} was critical for MED17 function, MED17 knockdown should have similar effects as S53A MED17 overexpression. Infection of HepG2 cells with MED17 shRNA adenovirus (Fig. 5D left) significantly decreased the mRNA abundance of *FASN* and other genes involved in lipogenesis, including *GPAM, ACC* and *SREBP1c*, but not those of oxidative genes (Fig. 5D right). To confirm that these effects were specifically due to the knockdown of MED17, we performed rescue experiments and detected significantly higher *FASN* mRNA abundance upon MED17 overexpression in these MED17 knockdown cells (Fig. S8C). In addition, administration of MED17 shRNA adenovirus in vivo (Fig. 5E left and middle) resulted in significantly reduced mRNA abundance of genes involved in lipogenesis, but not fatty acid oxidation (Fig. 5E right). Similar to the effect of MED17 S53A overexpression, knockdown of MED17 also resulted in significantly reduced FASN protein content (Fig. S9A). MED17 knockdown also resulted in lower abundance of nascent nuclear RNA for lipogenic genes, but not oxidative genes (Fig. 5F). In addition, the livers of MED17 knockdown mice showed a 20% reduction in newly synthesized palmitate (Fig. 5G left), reduced hepatic triglyceride amounts (Fig. 5F middle), and reduced Oil Red O staining (Fig. 5F right), showing that MED17 knockdown impaired lipogenesis, similar to expression of the phosphorylation defective S53A mutant. Overall, we conclude that MED17 and specifically phosphorylation of Ser^{53} in MED17 plays a critical role in the activation of lipogenic genes.

Author Manuscript Author Manuscript Author Manuscript Author Manuscript

We also examined whether phosphorylation of Ser^{53} in MED17 contributed to the dysregulation of lipogenic genes in obese leptin-deficient (*ob/ob)* mice. As has been previously documented, abundance of *FASN* mRNA in livers of fasted *ob/ob* mice was higher, but *FASN* mRNA abundance upon refeeding was similar between ob/ob and wild-type mice (Fig. S10B). Indeed, we detected higher Ser^{53} phosphorylation in livers of fasted *ob/ob* mice, while phosphorylation upon refeeding was similar in *ob/ob* and wild-type mice (Fig. S10A). However, CK2 protein content was similar between *ob/ob* and wild-type mice (Fig. S10A). Since the glucagon-PKA pathway is impaired in *ob/ob* mice during fasting (26), it is likely that phosphorylation of Ser^{53} in MED17 was higher due to lack of phosphorylation of Thr^{570} by the glucagon-PKA-p38 signaling axis.

To examine the role of CK2 in lipogenic gene induction, we administered CK2α1 shRNA adenovirus (Fig. 6A left and middle), which made the phosphorylation of Ser^{53} in MED17 undetectable (Fig 6A middle). Knockdown of CK2α1 decreased the mRNA abundance for lipogenic genes by 50–80% without affecting that for oxidative genes (Fig. 6A right), decreased FASN protein abundance by 40% (Fig. S9B), and decreased hepatic triglyceride content over 50% (Fig. 6B). Administration of the CK2 inhibitor CX-4945 resulted in a 60–80% reduction in the mRNA abundance for lipogenic genes upon refeeding without affecting that for oxidative genes (Fig. 6C) and decreased hepatic triglyceride content by 48% (Fig. 6D). Overall, our results demonstrated that CK2-mediated phosphorylation of Ser^{53} in MED17 was critical for feeding- and insulin-dependent transcription activation and induction of lipogenesis.

DISCUSSION

De novo lipogenesis is a complex and tightly regulated process that is closely tied to nutritional and hormonal status. Many enzymes in this pathway are regulated at the transcriptional level in a coordinate manner(4). We have previously established that USF1 is a key regulator of transcription for enzymes in lipogenesis, as it acts as a hub for various transcription factors and coregulators recruited for transcriptional activation upon insulin stimulation (12, 13, 27). We have shown that, although bound to *FASN* promoter under either fasting conditions or after feeding in mice or by the presence or absence of insulin in cells, USF1 is phosphorylated by DNA-dependent protein kinase (DNA-PK) at Ser^{262} in response to insulin, which is then acetylated at Lys^{237}. Moreover, BRG1-associated factor 60c (BAF60c) is phosphorylated by atypical protein kinase C (aPKC) at Ser^{247} upon insulin signaling, allowing interaction with acetylated USF1 for chromatin remodeling of lipogenic genes. However, how POL II and the general transcriptional machinery are recruited to the promoter regions of lipogenic genes in response to insulin were not known. Here we showed that USF1 directly interacted with and recruited a subunit of the Mediator complex, MED17, to the promoter regions of *FASN* and other lipogenic genes for activation in response to insulin. Moreover, we determined that: (i) MED17 was phosphorylated at Thr^{570} under serum starvation conditions and at Ser^{53} in response to insulin, (ii) MED17 promotion of lipogenic gene transcription depended on phosphorylation of Ser^{53} by CK2, and (iii) CK2 phosphorylated Ser^{53} in MED17 only in the absence of p38 MAPK-mediated phosphorylation of Thr^{570}. Thus we provided evidence for CK2 and phosphorylation of

Author Manuscript Author Manuscript Author Manuscript Author Manuscript

Ser^{53} in MED17 as an integral signaling component in transcriptional activation of lipogenesis in response to insulin.

Mediator acts as a bridge between gene-specific transcription factors and POL II and general transcriptional machinery. Although MED17 is indispensable in yeast (28), microarray analyses in mouse 3T3 fibroblasts have shown that knockdown of MED17 elicits changes in less than 5% of transcripts(29). That MED17 knockdown has such a restricted effect suggests that MED17 dependent recruitment of Mediator may be a feature of a subset of genes in mammalian cells that likely function in specific pathways. Our observation of a direct interaction between USF1 and MED17 coupled with increased MED17 recruitment to and activation of *FASN* and other lipogenic genes supports the notion that USF1-MED17 interaction plays a critical role in the transcription of lipogenic genes specifically in response to insulin.

We showed that CK2 phosphorylated Ser^{53} of MED17 to activate lipogenic genes, such as *FASN*, in response to insulin and that this phosphorylation is critical for the recruitment of MED17 to the *FASN* promoter in response to insulin. We also found that Thr^{570} phosphorylation that we detected in the absence of insulin was a target phosphorylation site of p38 MAPK, which is activated in fasting and a downstream signaling component of glucagon signaling(2, 21, 22). We found that CK2-mediated phosphorylation of Ser^{53} of MED17 was prevented by overexpression of T570D mutant. Thus, through the differential phosphorylation of MED17 at Ser^{53} and Thr^{570}, we linked CK2 to insulin-induced lipogenic gene transcription. CK2 is more active and abundant in white adipocytes than in brown adipocytes and it acts as an inhibitor of oxidation and energy expenditure(30).

In conclusion, transcriptional activation of genes involved in lipogenesis by USF1 in response to insulin requires multiple signaling pathways. We have previously identified two distinct pathways activated by phosphoinositide 3-kinase (PI3K) that contribute to USF-mediated transcriptional activation of lipogenic genes: Signaling through protein phosphatase 1 (PP1)/DNA-PK that posttranslationally modifies USF1, and signaling through aPKC/BAF60c to recruit USF1 to the BAF chromatin remodeling complex. Here, we showed a direct interaction between USF1 and MED17 and that, in the absence of Thr^{570} phosphorylation by p38 MAPK, MED17 was phosphorylated by CK2 at Ser^{53} in response to insulin and recruited Mediator to lipogenic gene promoters. Thus, we link POL II and the general transcriptional machinery to USF1, through the Mediator complex, for fatty acid and fat synthesis.

MATERIALS AND METHODS

Antibodies and siRNA

Rabbit polyclonal antibody was raised against a phospho-peptide corresponding to amino acids 38–56 of mouse MED17 (SQNLARLAQRIDFSQGSGSC) phosphorylated at Ser^{53}. The phospho-specific antibody was affinity purified before use. The following commercial antibodies were used: anti-FLAG (M2, Sigma), anti-phosphoserine (clone 4A4, Millipore), anti-CKII alpha (ab70774), anti-Pol II CTD phospho Ser^{2} (ab5095), anti-Pol II CTD phospho Ser^{5} (ab5408) (Abcam), anti-GAPDH (sc-25778), anti-HA-probe (sc-805), anti-

Author Manuscript Author Manuscript Author Manuscript Author Manuscript

CRSP77 (sc-12453), anti-MED6 (sc-366562), anti-MED7 (sc-12457), anti-MED15(sc-101185), anti-MED21(sc-101186), anti-MED25(sc-161112), anti-MED28(sc-104372), anti-USF1 (sc-229), anti-Pol II (sc-899) (SCBT), anti-Fatty Acid Synthase (sc-55580), and anti-TurboGFP (Thermo). siRNA for knockdown of USF1 in 293FT cells included: control siRNA (sc-37007) and USF1 siRNA (sc-36783) (SCBT).

Animal Experiments

Animal experiments were in compliance with the ethical regulations set by UC Berkeley Animal Care and Use Committee. Male C57BL/6 (wild type) mice (Jackson) or B6 Cg-Lep^{ob} (ob/ob) (Jackson) were used at 8 wks of age. Neither randomization nor blinding was employed. A sample size of 5 per group was initially used to assess whether differences could be detected and was found to be sufficient to achieve statistical significance. For fasting and refeeding experiments, mice were fasted overnight and then fed a high carbohydrate, fat free diet for 6 hrs. For knockdown or overexpression experiments, mice received through tail vein injection 100μl of adenovirus (MED17 shRNA, MED17 WT, MED17 S53A, or CK2α1 shRNA; Vector Biolabs) at 2.0×10^{10} PFU/mL. Twelve days after injection mice were fasted overnight then refed high carbohydrate diet for 6 hrs. Knockdown or overexpression was verified by measuring mRNA or protein abundance prior to qPCR analysis of lipogenic markers. For CK2 inhibition experiments, mice were injected with either vehicle or CX-4945 (75mg/kg; APEX Bio) intraperitoneally for 5 days, then fasted overnight and refed high carbohydrate diet for 6 hrs.

Cell Culture Experiments

HepG2 (ATCC) or HEK 293FT (Thermo) cells, grown in DMEM supplemented with 10% fetal bovine serum (FBS) and 100 units/mL of penicillin and streptomycin (P/S), were used for cell culture experiments. Cells were certified by the vendor and so were not authenticated before use. Cell lines were previously tested for mycoplasma and were found to be free of contamination. A sample size of 5 wells per group was initially used to assess whether differences could be detected. Experiments that did not achieve significant differences of $p<0.05$ were repeated with a larger sample size indicated in the figures legends. All cell culture experiments were replicated a minimum of 3 times. HepG2 cells were maintained in serum-free media overnight prior to treatment with 100 nM insulin for 30 min (for phosphorylation analysis), 8 hrs (for qPCR or ChIP-qPCR analyses), or 24 hrs (for triglyceride accumulation analyses). For CK2 inhibition studies, HepG2 cells were pretreated with 10 μM of CK2 inhibitor CX-4945 (Santa Cruz) for 30 min prior to insulin treatment. Adenovirus expressing MED17 shRNA, MED17 (WT), and MED17(S53A) (Vector Biolabs) were added to the growth medium HepG2 cells at a final concentration of 2.0×10^6 PFU/mL. After 48 hrs, infected HepG2 cells were switched to serum free media overnight then treated with insulin. 293FT cells in DMEM supplemented with 10% FBS and 100 units/mL of (P/S) were transfected with expression constructs using Lipofectamine 2000 (Invitrogen). For luciferase assays cells were transfected with 100 ng of each plasmid in 12-well plates. For coimmunoprecipitation and ChIP reactions, 293FT cells were transfected with 500 ng of each plasmid in 100 mm dishes.

Author Manuscript Author Manuscript Author Manuscript Author Manuscript

Chromatin immunoprecipitation

Livers from fasted or fed mice were homogenized and fixed with disuccinimidyl glutarate (DSG) at 2 mM in phosphate buffered saline (PBS) for 45 min at room temperature before 1% formaldehyde cross-linking/PBS for 10 min. The reaction was stopped with 125mM glycine for 5 min. Tissues were rinsed with ice-cold PBS 3 times and lysed in immunoprecipitation lysis buffer (500 mM HEPES, 1 mM EDTA, 140 mM NaCl, 0.5 % NP-40, 0.25 % Triton X-100, 5 % glycerol, and protease inhibitors) for 10 min at 4°C. Nuclei were collected by centrifugation at 600 × g for 5 min at 4°C. Nuclei were then lysed in nuclei lysis buffer (50mM Tris, 10 mM EDTA, 1% SDS, and protease inhibitors) and sonicated 8 times by 15 s bursts, each followed by 1 min cooling on ice. Chromatin samples were diluted 1:10 with dilution buffer (50 mM Tris, 10mM EDTA, 1% Triton-X100, and protease inhibitors). Soluble chromatin was quantified by absorbance at 260 nm, and equivalent amounts of input DNA were immunoprecipitated using 5–10 ug of indicated antibodies, or normal mouse IgG/normal rabbit IgG (Santa Cruz), and magnetic ChIP grade protein G beads (Cell Signaling). After the beads were washed and crosslinking was reversed, samples were treated with Proteinase K/RNAse A for 2 hrs, and DNA fragments were extracted with QIAquick columns (Qiagen). DNA was quantified with qPCR with the appropriate primers (table S1) to determine enrichment.

For re-ChIP experiments, 25uL of elution buffer (1% Triton-X, 10 mM Tris-HCl, 1mM EDTA, 150 mM NaCl, 10 mM DTT) was added to beads after the first phase of washes and samples were left at 37°C for 30 min. Eluates were transferred to new tubes and diluted to a final volume of 1mL in dilution buffer (1% Triton-X, 10 mM Tris-HCl, 1 mM EDTA, 150 mM NaCl) and incubated with the second antibody and protein G beads. Beads were then washed again, crosslinking was reversed, samples were treated with Proteinase K/RNAse A, and DNA was extracted with QIAquick columns (Qiagen). DNA was quantified with qPCR with the appropriate primers (table S1) to determine enrichment.

In vitro phosphorylation assays

6x-His-tagged MED17 (WT), MED17 (S53A), MED17 (S55A), and MED17 (T570A) were bacterially synthesized, then purified using nickel magnetic beads (Millipore). For analysis of phosphorylation by CK2, WT, S53A, and S55A proteins were incubated with or without CK2 (New England Biolabs), and with or without CX-4945, in kinase buffer (50 mM Tris, 10 mM $MgCl_2$, 0.1 mM EDTA, 2 mM DTT, 0.01% Brij) supplemented with 300 uM ATP at 25°C for 1 hr and the reaction was terminated by adding 20 uL of 2xSDS sample buffer. Reaction mixtures were separated by SDS-PAGE for immunoblotting and staining. For analysis of phosphorylation by p38 MAPK, wild-type and T570A proteins were incubated with or without p38 (SignalChem) in kinase buffer (25 mM MOPS, pH 7.2, 12.5 mM β-glycerol-phosphate, 25 mM $MgCl_2$, 5 mM EGTA, 2 mM EDTA, 0.25 mM DTT) supplemented with 300 uM ATP at 30°C for 1 hr and the reaction was terminated by adding 20 uL of 2x SDS sample buffer. Reaction mixture was separated by SDS-PAGE for immunoblotting.

Author Manuscript Author Manuscript Author Manuscript Author Manuscript

Immunoprecipitation, GST pull-down, and luciferase reporter assays

For immunoprecipitation analyses, nuclear extracts were collected as described previously (13) and were diluted with 1% Triton-X in PBS and incubated with the specific antibodies overnight at 4°C followed by addition of protein G agarose beads (Santa Cruz). The immunoprecipitates were separated by SDS-PAGE and proteins were transferred onto nitrocellulose membranes (BioRad) for immunoblotting. For GST pulldown, bacterially expressed GST-USF-1 fusion protein on glutathione-agarose beads (Santa Cruz) were incubated with ^{35}S labeled MED17 protein. The proteins were separated by SDS-PAGE before autoradiography. For His-tag pulldown, bacterially expressed 6xHis-MED17 fusion proteins on nickel magnetic beads (Millipore) were incubated with in vitro translated USF. The proteins were separated by SDS-PAGE before immunoblotting. 293FT cells were transfected with 444-*FASN* promoter-luciferase along with various expression constructs using Lipofectamine 2000 (Invitrogen), and luciferase assays were performed using Dual-Luciferase Reporter Assay (Promega).

Mass spectrometric analysis

Site specific phosphorylation of proteins was detected by enzymatically digesting purified protein mixture and subjecting digested peptides to 2D “MudPIT” Run (cation exchange/RP LC-MS/MS) using a Thermo LTQ XL mass spectrometer. DTA select program was used to interpret the mass spectra.

RT-qPCR analysis

Total RNA was isolated using Trizol reagent (Gibco) and reverse transcribed. cDNAs were amplified by qPCR using 7500 Fast Real-time PCR system (ABI Applied Biosystems). Relative mRNA abundance was quantified using GAPDH as a control. Statistical analysis of the qPCR was obtained using the TMCt method.

Preparation of nascent RNA

Nuclei from mouse livers were isolated by centrifugation through sucrose cushion as described previously (33). Nuclei were treated with DNAse (Roche) and purified using RNeasy kit (Qiagen).

Measurement of de novo lipogenesis

Fatty acids synthesized during a 24-hr $^{2}H_2O$ body water labeling period were measured. Mass isotopomer distribution analysis (MIDA) was performed. Fractional DNL contribution was calculated as previously described by $f\mathrm{DNL}=\mathrm{EM1}_{\mathrm{FA}}/\mathrm{A1}_{\mathrm{FA}}$ (34).

Measurement of Triglyceride content

Total neutral lipids were extracted by the Folch method and were solubilized in 1% Triton X-100. Triglyceride content was measured with Infinity Reagent (Thermo).

Statistical Analysis

The data are expressed as the means ± standard errors, and a Wilcoxon Rank-Sum test was used to test difference between single comparisons. Data where multiple comparisons are

Author Manuscript Author Manuscript Author Manuscript Author Manuscript

being made were tested with the Wilcoxon Rank-Sum test and the Holm correction was applied. The Holm correction was applied to each experiment independently.

Supplementary Material

Refer to Web version on PubMed Central for supplementary material.

Acknowledgments

FUNDING: This work was supported by RO1DK081098 (NIH) to HSS. JAV was supported by F32DK105671 (NIH). The mass spectrometric analysis was performed at the Vincent J. Proteomics/Mass Spectrometry Laboratory at UC Berkeley, which was supported by S10RR025622 (NIH).

REFERENCES AND NOTES

1. Wong RHF, Sul HS. Current Opin Pharmacol. 2010; 10:684.
2. Cao W, et al. J Biol Chem. Dec 30.2005 280:42731. [PubMed: 16272151]
3. Paulauskis JD, Sul HS. J Biol Chem. May 25.1988 263:7049. 1988. [PubMed: 2452820]
4. Paulauskis JD, Sul HS. J Biol Chem. Jan 5.1989 264:574. 1989. [PubMed: 2535847]
5. Wang D, Sul H. J Biol Chem. 1998; 273:25420. [PubMed: 9738010]
6. Wang D, Sul H. J Biol Chem. 1997; 272:26367. [PubMed: 9334210]
7. Wang D, Sul H. J Biol Chem. 1995; 270:28716. [PubMed: 7499393]
8. Moustaïd N, Beyer RS, Sul HS. J Biol Chem. Feb 25.1994 269:5629. 1994. [PubMed: 8119899]
9. Moon Y, Latasa M, Kim K, Wang D, Sul H. J Biol Chem. 2000; 275:10121. [PubMed: 10744693]
10. Latasa MJ, Griffin MJ, Moon YS, Kang C, Sul HS. Mol Cell Biol. Aug 15.2003 23:5896. 2003. [PubMed: 12897158]
11. Casado M, Vallet VS, Kahn A, Vaulont S. J Biol Chem. Jan 22.1999 274:2009. 1999. [PubMed: 9890958]
12. Wang Y, et al. Mol Cell. 2013; 49:283. [PubMed: 23219531]
13. Wong RHF, et al. Cell. 2009; 136:1056. [PubMed: 19303849]
14. Allen BL, Taatjes DJ. Nat Rev Mol Cell Biol. 2015; 16:155. [PubMed: 25693131]
15. Knuesel MT, Taatjes DJ. Transcription. 2011; 2:28. 2011/01/01. [PubMed: 21326907]
16. Lacombe T, Poh SL, Barbey R, Kuras L. Nucleic Acids Res. 2013; 41:9651. [PubMed: 23963697]
17. Kim S, Gross DS. J Biol Chem. Apr 26.2013 288:12197. 2013. [PubMed: 23447536]
18. Fan X, Chou DM, Struhl K. Nat Struct Mol Biol. 2006; 13:117. [PubMed: 16429153]
19. Imasaki T, et al. Nature. 2011; 475:240. [PubMed: 21725323]
20. Xue Y, et al. Protein Eng Des Sel. Mar 1.2011 24:255. 2011. [PubMed: 21062758]
21. Chen J, Ishac EJ, Dent P, Kunos G, Gao B. Biochem J. Sep 15.1998 334:669. [PubMed: 9729476]
22. Longuet C, et al. Cell Metab. Nov.2008 8:359. [PubMed: 19046568]
23. Meggio F, Pinna LA. FASEB J. Mar 1.2003 17:349. 2003. [PubMed: 12631575]
24. Litchfield DW. Protein kinase CK2: structure, regulation and role in cellular decisions of life and death. 2003; 369:1–15.
25. Heidemann M, Hintermair C, Voß K, Eick D. BBA - Gene Regul Mech. 2013; 1829:55.
26. VINE RLL, VOYLES N, PERRINO PV, RECANT L. Endocrinology. 1975; 97:615. [PubMed: 170069]
27. Griffin MJ, Wong RHF, Pandya N, Sul HS. J Biol Chem. Feb 23.2007 282:5453. 2007. [PubMed: 17197698]
28. Takagi Y, Kornberg RD. J Biol Chem. Jan 6.2006 281:80. 2006. [PubMed: 16263706]
29. van Essen D, Engist B, Natoli G, Saccani S. PLoS Biol. 2009; 7:e1000073.
30. Shinoda K, et al. Cell Metab. 2015; 22:997. [PubMed: 26525534]

Author Manuscript Author Manuscript Author Manuscript Author Manuscript

31. Olsen B, Wang SY, Svenstrup T, Chen B, Guerra B. BMC Molecular Biol. 2012; 13:1.
32. Sanchez-Casalongue ME, et al. J Biol Chem. Mar 13.2015 290:7221. 2015. [PubMed: 25631054]
33. Paulauskis JD, Sul HS. J Biol Chem. Jan 5.1989 264:574. [PubMed: 2535847]
34. Ahmadian M, et al. Cell Metab. 2011; 13:739. [PubMed: 21641555]

Author Manuscript
Author Manuscript
Author Manuscript
Author Manuscript

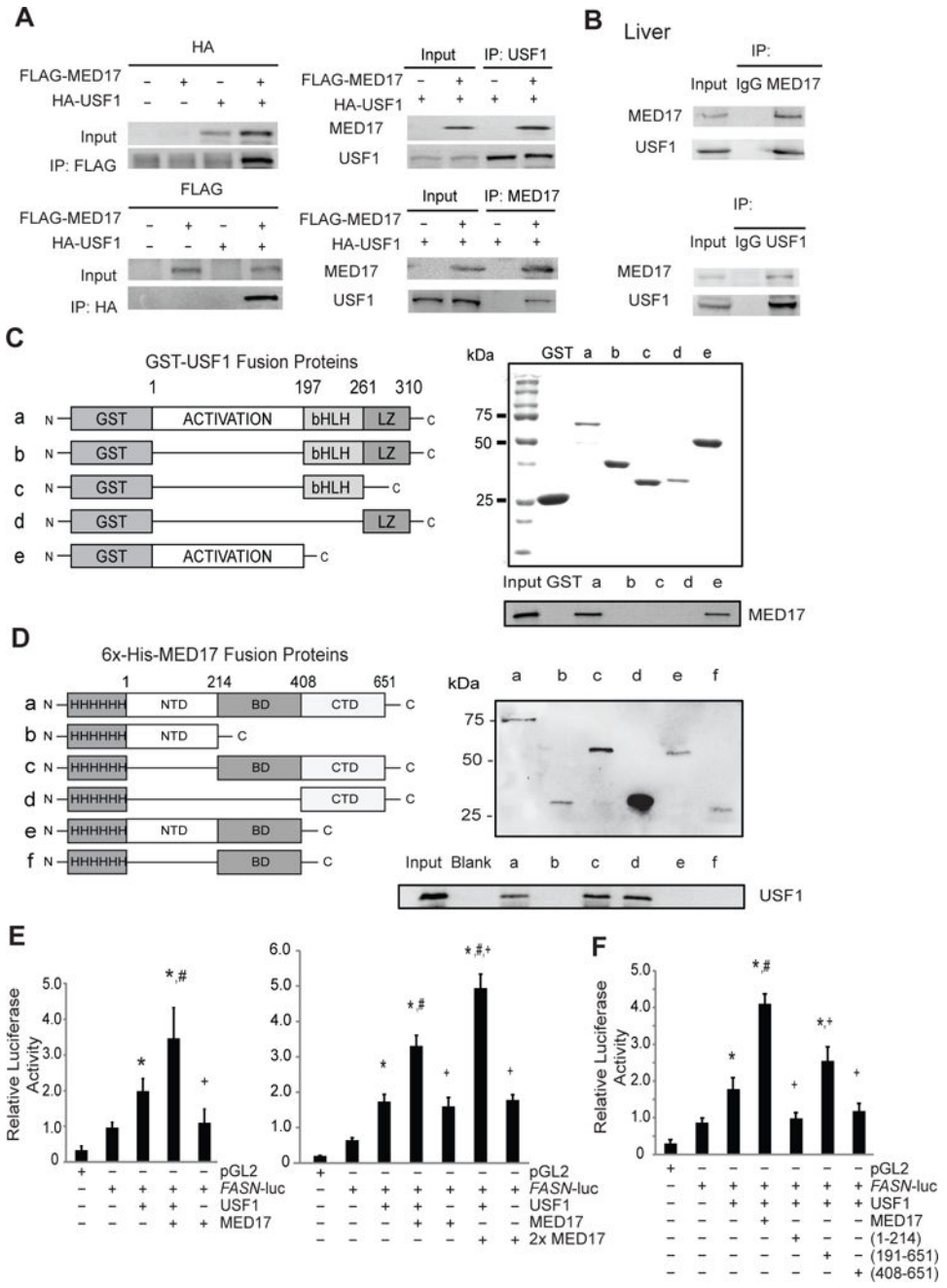

Fig. 1. USF1 directly interacts with MED17

(A) Immunoblot (IB) of proteins from coimmunoprecipitation (Co-IP) of 293FT cells overexpressing FLAG-tagged MED17 (75kDa) and HA-tagged USF1 (37kDa). n=6 independent experiments.

(B) IB of proteins from Co-IP of liver nuclear extracts using either MED17 or USF1 antibodies. n=6 independent experiments.

(C) Diagram of USF1 deletion constructs (left). GST-USF1 proteins in bacterial cell lysates were detected by Coomassie staining (right, top). GST-pulldown assays were performed

Author Manuscript Author Manuscript Author Manuscript Author Manuscript

with GST-USF1 proteins and ^{35}S-labeled MED17 (right, bottom). n=5 independent experiments.

(D) Diagram of MED17 deletion constructs (left). 6xHis-MED17 proteins in bacterial cell lysates were detected by immunoblotting (right, top). His-tag pulldown assays were performed with 6xHis-MED17 proteins and ^{35}S-labeled USF1 (right, bottom). n=5 independent experiments.

(E–F) *FASN* promoter activity in 293FT cells overexpressing the indicated proteins (Means ±SEM).* different from *FASN* at $p<0.05$, # different from *FASN* + USF1 at $p<0.05$, + different from *FASN* + USF1 + MED17 at $p<0.05$. n=6 wells of cells per group.

Author Manuscript Author Manuscript Author Manuscript Author Manuscript

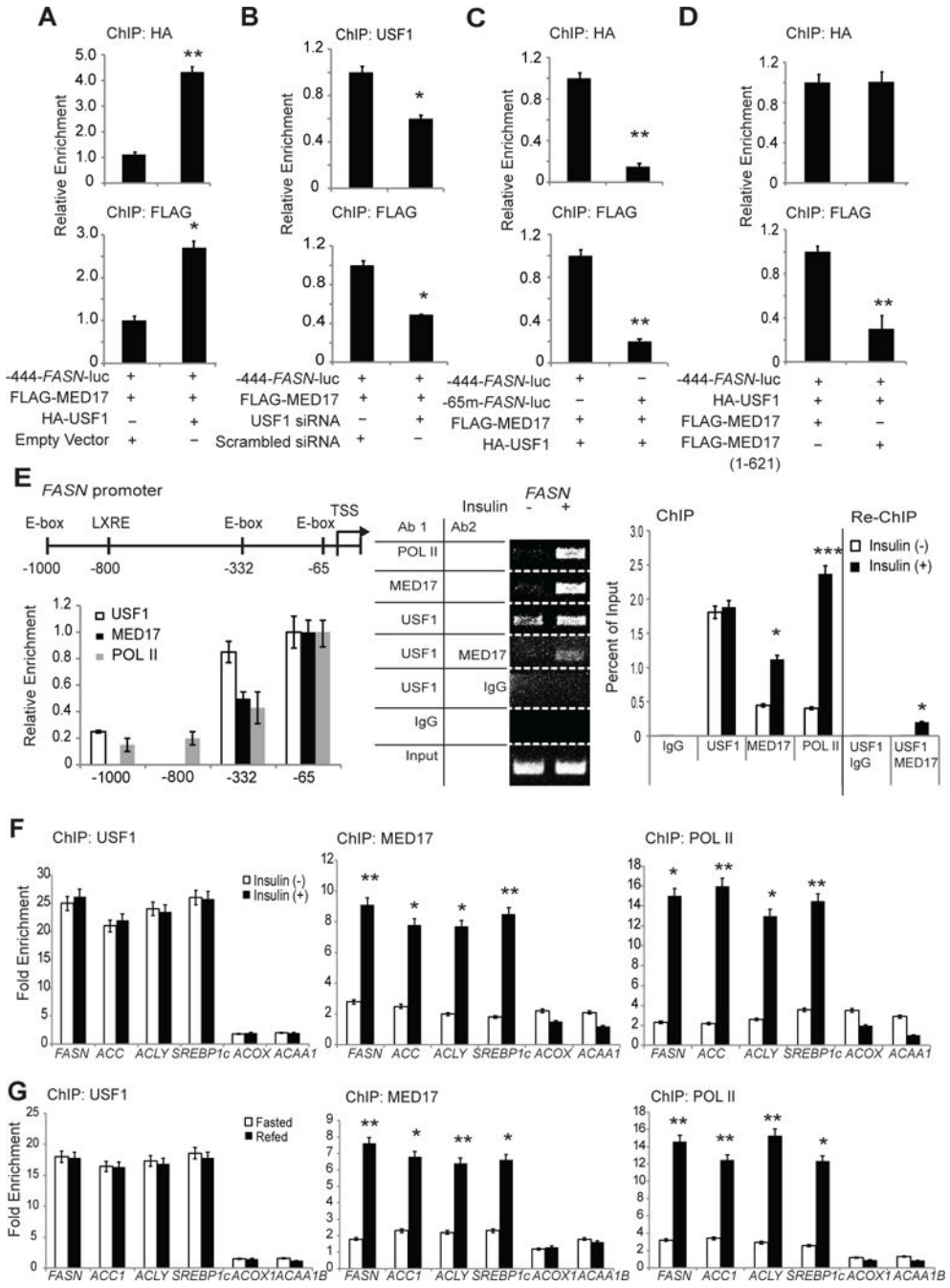

Fig. 2. MED17 is recruited to the *FASN* promoter in a feeding and insulin dependent manner

(A–D) ChIP using the indicated antibodies of 293FT cells transfected with indicated vectors. n=5 wells of cells per group. A) Cells were transfected with -444-*FASN*-luc, FLAG-MED17, and either HA-USF1 or empty vector. B) Cells were transfected with -444-*FASN*-luc, FLAG-MED17, and either USF1 siRNA or scrambled siRNA. C) Cells were transfected with FLAG-MED17, HA-USF1, and either -444-*FASN*-luc or -65m-*FASN*-luc. D) Cells were transfected with -444-*FASN*-luc, HA-USF1, and either FLAG-MED17 (WT) or FLAG-MED17 (1-621).

Author Manuscript Author Manuscript Author Manuscript Author Manuscript

(E) Map of the HepG2 *FASN* promoter region showing the relative enrichment of USF1, MED17, and POL II (left). Agarose gel image of Re-ChIP of *FASN* promoter in HepG2 cells (middle) and quantification by qPCR (right) using primers targeting the -65-E-box region. n=5 dishes of cells per group.
(F) ChIP-qPCR of fatty acid synthetic and oxidative promoters in HepG2 cells using the indicated antibodies. n=5 dishes of cells per group.
(G) ChIP-qPCR analysis of fatty acid synthetic and oxidative promoters in livers of fasted and refed mice. n=5 mice per group.
(A–G) Means ±SEM. *p<0.05, **p<0.01, ***p<0.001.

Author Manuscript Author Manuscript Author Manuscript Author Manuscript

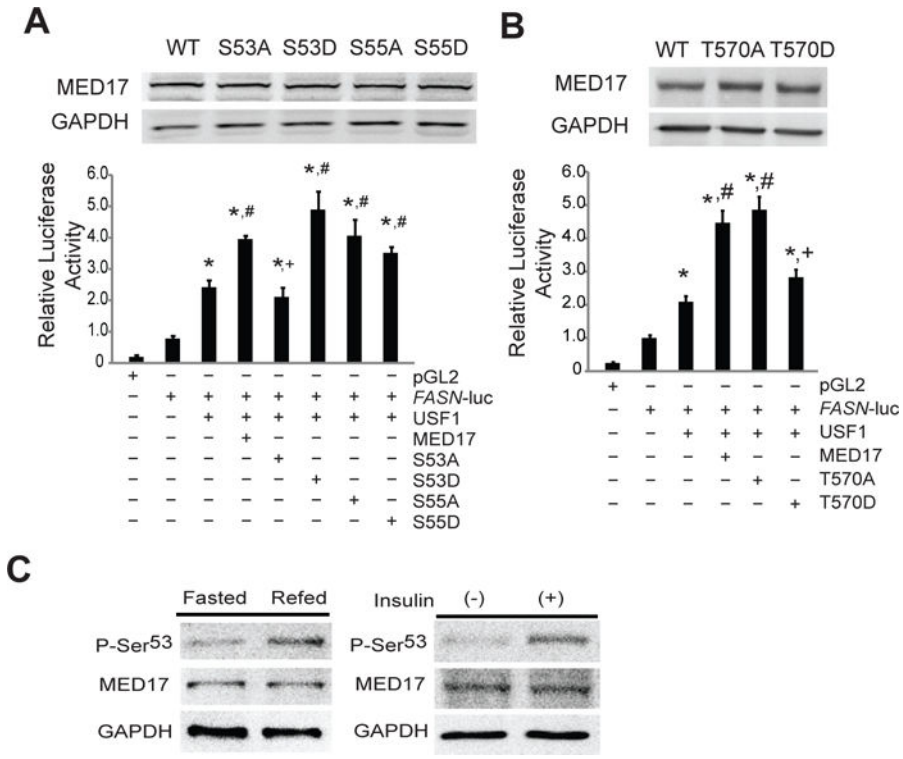

Fig. 3. Differential phosphorylation of MED17 is required for *FASN* promoter activation

(A–B) *FASN* promoter activity and representative blots of 293FT cells transfected with the indicated vectors. * different from *FASN* at $p<0.05$, # different from *FASN* + USF1 at $p<0.05$, + different from *FASN* + USF1 + MED17 at $p<0.05$. n=8 wells of cells per group for (A) and n=5 wells of cells per group for (B).

(C) IB of immunoprecipitated MED17 from nuclear extracts of livers from fasted or refed mice (n=5 mice per group) or serum-starved or insulin-treated HepG2 cells (n=4 independent experiments) using P-Ser^{53} and total MED17antibodies.

Author Manuscript Author Manuscript Author Manuscript Author Manuscript

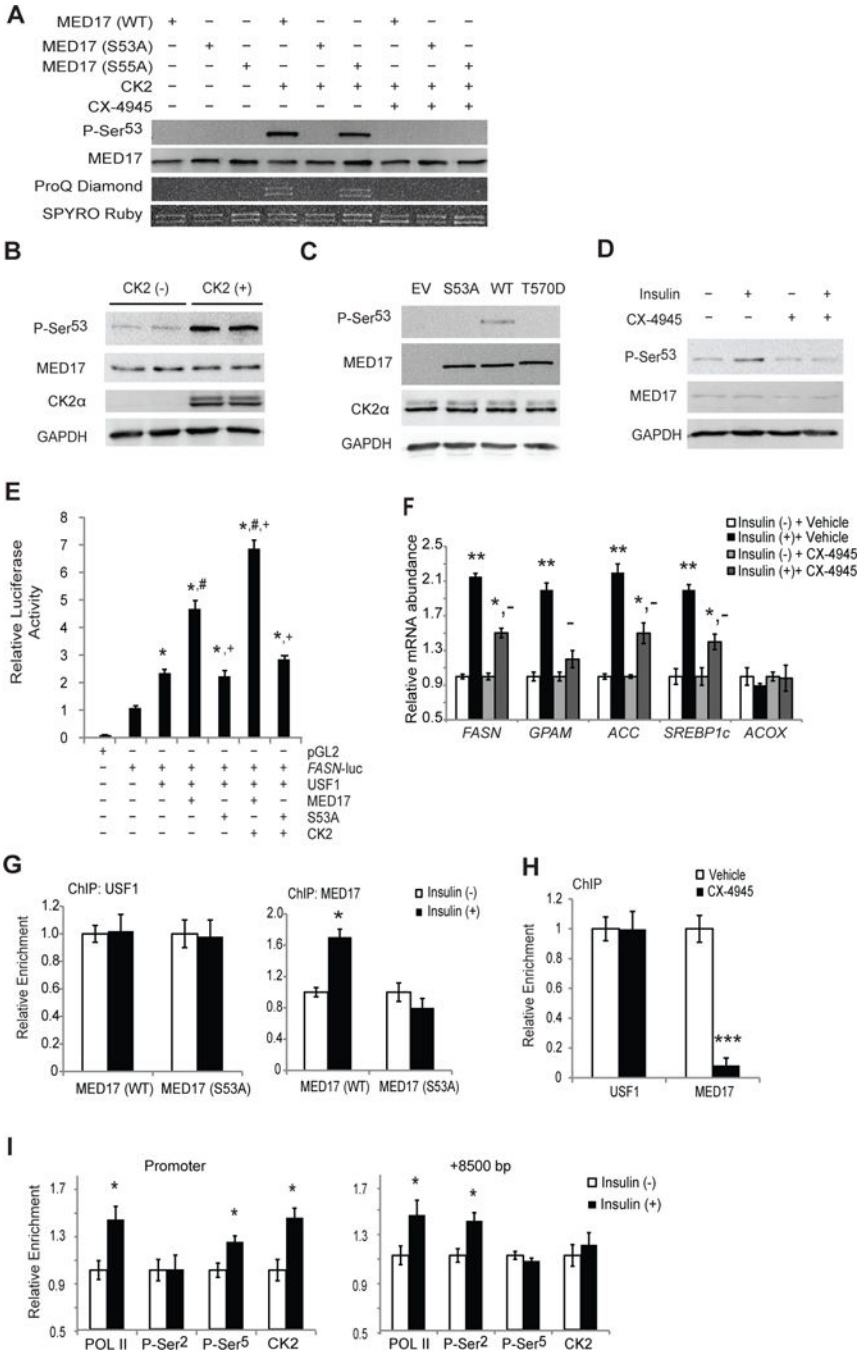

Fig. 4. CK2-mediated phosphorylation of MED17 at Ser^{53} is required for its recruitment and activation of *FASN* promoter in response to insulin

(A) In vitro phosphorylation assays with WT, S53A or, S55A forms of MED17 and recombinant CK2. Reactions were separated by SDS-PAGE and either immunoblotted with the indicated antibodies or stained with phosphospecific or total protein dye. n=4 independent experiments.

(B) IB of 293FT cells overexpressing MED17. Cells were transfected with either empty vector or CK2α and β. Cells were immunoblotted using antibodies against P-Ser^{53}, MED17 (75 kDa), and CK2α (45 kDa). n=5 independent experiments.

Author Manuscript Author Manuscript Author Manuscript Author Manuscript

(C) IB of 293FT cells transfected with CK2α and β, and WT, S53A or T570D forms of MED17. n=4 independent experiments.
(D) IB of HepG2 cells that were serum-starved overnight, pretreated with CX-4945 or vehicle for 30 mins, and then treated with insulin for 30 mins. n=5 independent experiments.
(E) *FASN* promoter activity in 293FT cells overexpressing the indicated proteins (Means ±SEM)* different from *FASN* at $p<0.05$, # different from *FASN* + USF1 at $p<0.05$, + different from *FASN* + USF1 + MED17 at $p<0.05$. n=8 wells of cells per group.
(F) qPCR of HepG2 cells that were serum-starved, pre-treated with CX-4945, and then treated with insulin (Means ±SEM, * different from (−) Insulin + Vehicle at $p<0.05$, **$p<0.01$; − different from (+) Insulin + Vehicle at $p<0.05$). n=7 wells of cells per group.
(G) ChIP-qPCR of the *FASN* promoter from HepG2 cells infected with MED17(WT) or MED17(S53A) adenovirus. n=5 dishes of cells per group.
(H) ChIP-qPCR of HepG2 cells serum starved overnight, then pretreated with CX-4945 for 30 min prior to 8 hr treatment with insulin. n=5 dishes of cells per group.
(I) ChIP-qPCR of chromatin from serum-starved/insulin treated HepG2 cells at the *FASN* proximal promoter region and 8500 bp downstream of the transcription start site. n=5 dishes of cells per group.
(G–I) Means ±SEM, *$p<0.05$,***$p<0.001$.

Author Manuscript Author Manuscript Author Manuscript Author Manuscript

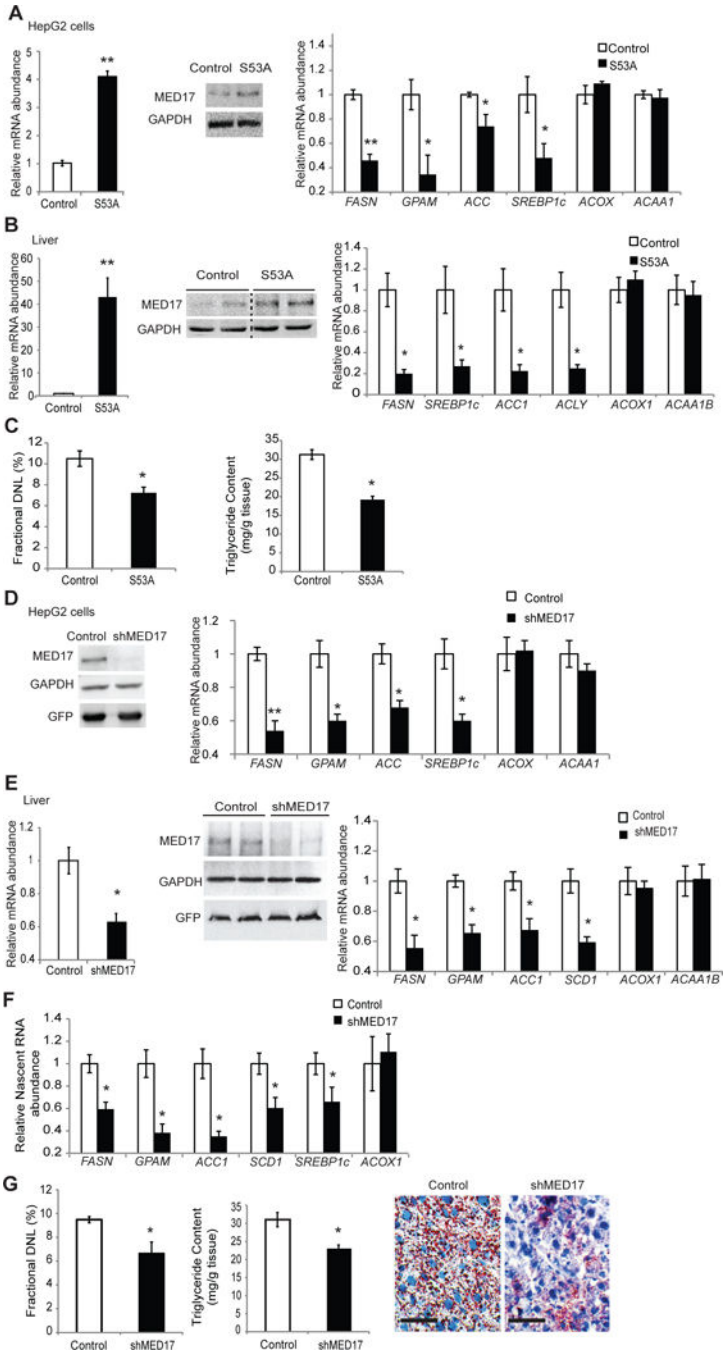

Fig. 5. Phosphorylation of Ser^{53} in MED17 is required for lipogenesis by insulin in vivo

(A–B) *MED17* mRNA abundance (left) and representative blots (middle) in HepG2 cells (A; n= 5 dishes of cells per group) or livers of mice (B; n= 5mice per group) after infection with either control adenovirus or Ad-MED17-S53A. mRNA abundance of the indicated genes (right). Dashed lines indicate image splicing to remove unnecessary lanes.

(C) Percent of newly synthesized palmitate (left), and hepatic triglyceride content (right) in livers of control adenovirus or Ad-MED17-S53A infected mice (n=5 mice per group).

Author Manuscript Author Manuscript Author Manuscript Author Manuscript

(D) Representative blot of MED17 after infection of HepG2 cells with either control adenovirus or Ad-shMED17 for MED17 knockdown (left). mRNA abundance of the indicated fatty acid synthetic or oxidative genes (right) (n=5 dishes of cells per group).
(E) MED17 mRNA abundance (left) and representative blot (middle) from livers of mice injected with either control or Ad-shMED17 adenovirus. mRNA abundance of the indicated fatty acid synthetic or oxidative genes (right) (n=5 mice per group).
(F) Nascent RNA abundance of FA synthetic or oxidative genes (n=5 mice per group)
(G) Percent of newly synthesized palmitate (left), hepatic triglyceride content (middle), and representative images Oil Red O staining with 50 μm scale bars (right) (n=5 mice per group) of livers from mice administered control or shMED17 adenovirus.
(A–G) Means ±SEM, *$p<0.05$, **$p<0.01$.

Author Manuscript Author Manuscript Author Manuscript Author Manuscript

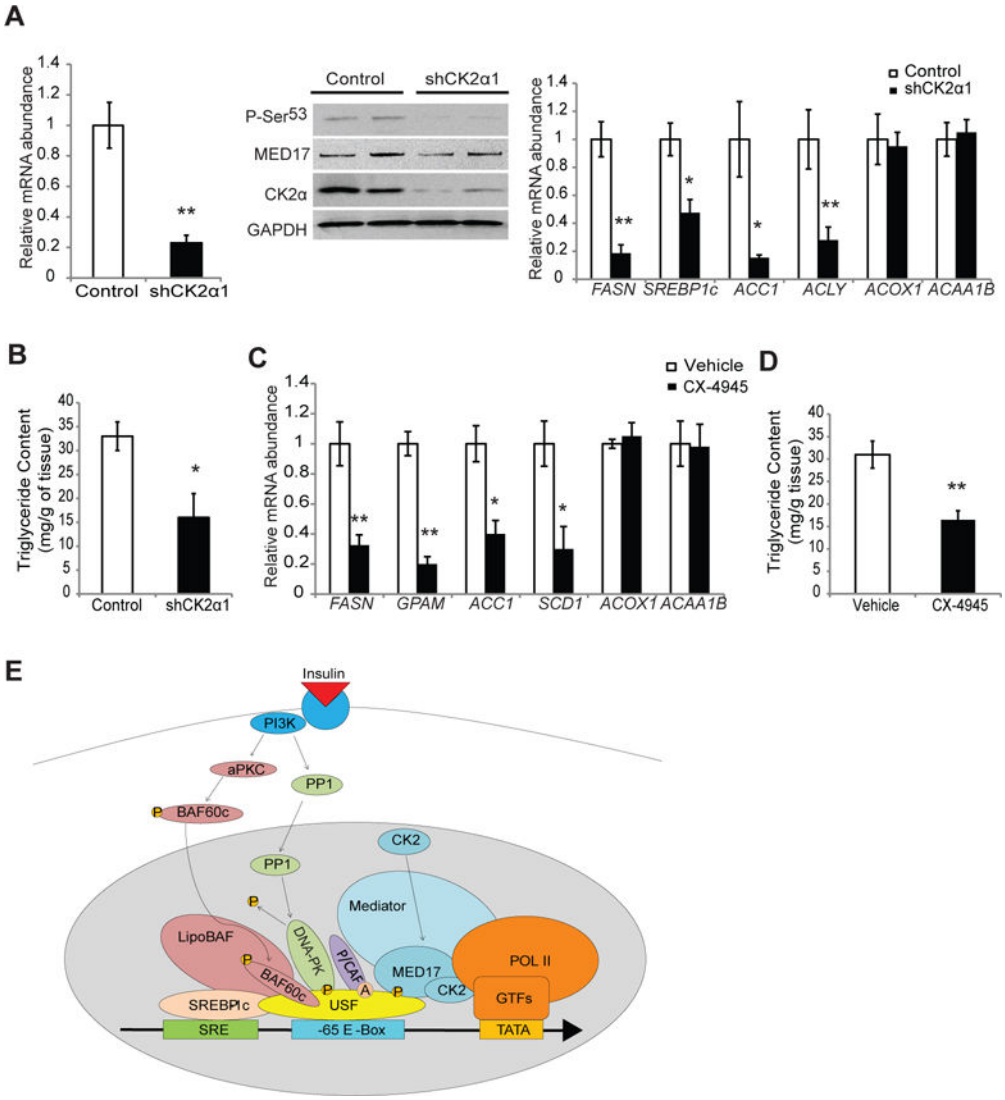

Fig. 6. CK2 phosphorylates MED17 to promote lipogenesis in response to insulin in vivo

(A) *CK2α1* mRNA abundance (left) in livers from mice injected with control adenovirus or Ad-shCK2α1. Representative blot of MED17 and CK2α1 (center). mRNA abundance of fatty acid synthetic or oxidative genes (right) (n=5 mice per group).

(B) Hepatic triglyceride content of mice infected with either control adenovirus or Ad-shCK2α1 (n=5 mice per group).

(C) mRNA abundance for the indicated genes from livers of mice treated with either vehicle or the CK2 inhibitor CX-4945(n=5 mice per group).

(D) Hepatic triglyceride content in mice treated with either vehicle or CX-4945(n=5 mice per group).

(A–D) Means ±SEM, *p<0.05, **p<0.01.

(E) Insulin signaling pathways for USF1-mediated transcriptional activation of lipogenesis through recruitment of coregulators, Mediator complex, and POL II and general transcription machinery.